Egyptian Journal of Aquatic Biology & Fisheries
Zoology Department, Faculty of Science,
Ain Shams University, Cairo, Egypt.
ISSN 1110 – 6131
Vol. 28(6): 497 – 518 (2024)
www.ejabf.journals.ekb.eg

Gametogenesis and Reproduction Cycle of the Burrowing Urchin *Echinometra mathaei* (Echinodermata: Echinoidea) from the Northern Red Sea

Mohamed M. Rashad[1*], Hany A. Abdel-Salam[2], Mohammed Salem[3], Saad Z. Mohamed[4], Nesreen K. Ibrahim[4]

[1]Marine Ecology Department, Faculty of Aquaculture and Marine Fisheries, Arish University, Egypt
[2]Zoology Department, Faculty of Science, Benha University, Benha, Egypt
[3]Marine Fsheries Department, Faculty of Aquaculture and Marine Fisheries, Arish University, Egypt
[4]Marine Science Department, Faculty of Science, Suez Canal University, Ismallia, Egypt
[*]**Corresponding Author: mohamed.rashad@aqua.aru.edu.eg**

ARTICLE INFO

Article History:
Received: Nov. 2, 2024
Accepted: Nov. 16, 2024
Online: Nov. 17, 2024

Keywords:
Echinometra mathaei,
Gametogenesis,
Ultra-structure,
Developmental stages,
Global warming,
Northern Red Sea

ABSTRACT

The burrowing sea urchin *Echinometra mathaei* (Blainville, 1825) is a common species found on reefs in the tropical regions of the Indo-Pacific Ocean, typically at depths of up to 139 meters. The gametogenesis and reproductive strategy of the *E. mathaei* population were investigated at two study sites: Al-Ain Al-Sukhna public beach and Hurghada in the northern Red Sea, from spring 2023 to winter 2024. To examine sexual differences in gonadal maturation, histological sections of *E. mathaei* gonads were analyzed. At the first site, reproductive activity peaked in late summer and continued into autumn, while at the second site, fully mature oocytes were observed year-round. Following laboratory induction of spawning, the fertilization rate increased to 90%, reaching the prism stage. Environmental factors, such as temperature and salinity, were found to affect reproductive state and gonadal development. Sea water temperatures rose in summer 2023, coinciding with an increase in gamete size at both study sites. The diameters of oocytes and spermatocytes reached their maximum values in autumn (532.01 and 170.38µm at the first site; 535.4 and 170.21µm at the second site). These results indicate that temperature is a significant factor influencing the gametogenesis processes.

INTRODUCTION

Echinometra mathaei (Blainville, 1825) extends from the East African coast and the Red Sea to Hawaii **(Andreas, 2010)**. It is globally acknowledged as the most prevalent sea urchin species **(Metz *et al*., 2020)** and is commonly found in tropical and sub-tropical regions **(Ahmed *et al*., 2023)**. It has an important role in maintaining population stability, nutrient cycling, and habitat modification within coral reef ecosystems **(McClanahan & Muthiga , 2020)**. By grazing on macroalgae, *E. mathaei* helps maintain a balance between algal populations and corals, thereby promoting coral health and preventing excessive algal growth **(Angellia & Nugrahapraja, 2023)**.

The reproductive process of burrowing sea urchin includes nutrient storage, proliferation of gametes and their maturation. Initially, the gonads expand as they store nutrients. Subsequently, gametogenic cells undergo growth and maturation, leading to the production of mature ova and spermatozoa within the gonadal cavity, with minimal nutritive substances remaining at this stage **(Siddique & Ayub, 2019)**.

Echinoderms display different reproductive patterns based on latitude. Polar and high-latitude species show distinct reproductive seasonality **(Grange, 2005)**, while this seasonality decreases in mid-latitude species **(Rubilar *et al.*, 2005)**. Moreover, it is absent in tropical species **(Guzmán & Guevara, 2002)**. Reproductive activity is influenced by the increasing seasonality from the tropics to the poles **(Byrne *et al.*, 1998)**.

The reproductive cycles of *E. mathaei* were investigated in various coastal areas like northwest Red Sea **(Hernandez, 2019)**, Rottnest Island **(Campbell & Gusman, 2020)**, and Hawaii **(Nishihira *et al.*, 2020)**. **Pearse and Cameron (1991)** observed that in certain tropical areas near the equator, breeding occurs year-round, where environmental factors, especially temperature, are presumed to be more stable. However, in more distant locations, spawning is confined to specific periods.

The reproductive cycle of echinoids, including gametogenesis, is predominantly influenced by various environmental factors such as seasonal changes in photoperiod, water temperature, phytoplankton blooms, lunar periodicity, food availability, and population density **(Martínez-Pita *et al.*, 2010; Hernández *et al.*, 2011; Pecorino *et al.*, 2014; Hasan, 2019)**.

This study aimed to provide a comprehensive description of the gametogenesis and reproductive strategy of the *E. mathaei* population by conducting histological analysis of gonadal development in the Egyptian waters of the northern Red Sea. The studied urchin is commonly found along the rocky coasts. This research is considered to be the first work investigating the early developmental stages by using induce spawning. Additionally, it reported the potential influence of seawater temperature and salinity on the reproductive cycle of the study urchin.

MATERIALS AND METHODS

Study area

The study was conducted at two different sites along the northern part of the Red Sea.

Al-Ain Al-Sukna (Site I)

Al-Ain Al-Sukhna is a public beach on the northwestern coast of the Gulf of Suez, Red Sea ($29^{o}\,33^{'}\,20.7"$ & $32^{o}\,21^{'}\,44.8^{"}$ E) (Fig. 1). It is characterized by a high distribution

and diversity of sea urchin species, in addition to a decline in coral reef coverage. It's a rocky site at the coastline followed with a sandy bottom that extends for 54m and batches of coral reefs, which are facing a bleaching event because of the increasing sea water temperature and high human activity **(Ali *et al*., 2011)**.

Hurghada (Site II)

It is extending from the Hurghada's youth hostel beach to the northern west of the National Institute of Oceanography and Fisheries (27º 17'07.5" & 33º 46' 11.8" E) (Fig. 1). This site is characterised by a rocky beach at the Hurghada's youth hostel, followed by a sandy bottom with vertical coral batches, while the northern-west part of NIOF is characterized by a sandy beach, followed by vertical coral reefs with high coverage of seagrass.

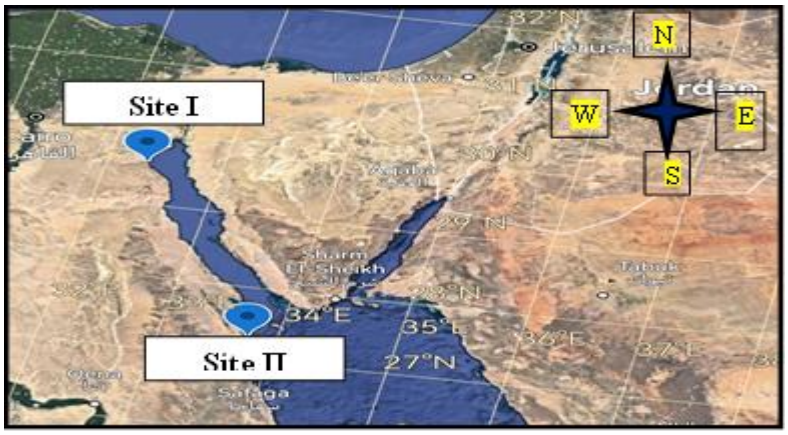

Fig. 1. A map of the northern Red Sea showing the study sites. Al-Ain Al-Sukna (site I) and Hurghada (site II)

Sampling

Samples of the studied sea urchin *Echinometra mathaei* were seasonally collected from spring 2023 to winter 2024. They were hand-picked at depths between three to five meters. The sea urchin samples were placed in polyethylene plastic aquaria filled with seawater and immediately transferred to well-aerated and sunlit aquaria settled at Marine Genomics Laboratory of Benha University, Benha City. These aquaria were filled with natural seawater, and the temperature of seawater was adjusted at an appropriate temperature according to the sampling time. Samples of *E. mathaei* were photographed in the field and in the aquaria using a high resolution digital camera.

Physico-chemical parameters

The physico-chemical parameters of seawater, temperature and salinity were measured at the two investigated sites by Hydrolab HANNA GPS Multiparameter Meter (HI 9829).

Histological studies

Samples from the gonad from the sea urchin's aboral tip were fixed in 10% formalin for 24 hours (**Ibrahim *et al.*, 2021**) and then transferred to 70% alcohol for further processing. Dehydration and infiltration processes were applied to the gonad samples before embedding them in paraffin wax. The samples were then sectioned at a thickness between 5 to 7μm using a PR-5014 rotary microtome. Sections were stained with Delafield's Haematoxylin and counterstained with Eosin **(Madhavi *et al.*, 2000)**.

Male and female gonads were categorized into four gametogenetic stages, which represented variations in both the nutritive phagocyte (NP) and germ cell populations. These stages were identified as follows: Stage I: Immature (Inter-gametogenesis and NP phagocytosis), stage II: Intiation of gametogenesis, stage III: Mid-gametogenesis and NP utilization), and stage IV: End of gametogenesis (NP exhaustion, and spawning). The partially spawned and spent individuals were grouped together to determine the spawning season in male and female sea urchins.

Furthermore, correlations between spawning and environmental factors (temperature and salinity) were calculated by using the software package SPSS.

Oocytes diameter

The diameter of oocytes at various developmental stages in females were measured through microscopic analysis of histological sections using an ocular micrometer at the widest part of the oocytes. Each section was divided into three subsamples of 2.5mm area, with three replicates.

Induce spawning and fertilization

Sea urchins weighing between 40 and 85 grams were carefully selected for induced spawning. A volume of 1.5 to 2ml of 0.5 M potassium chloride (KCl, pH 6.1) was administered to the animals via injection on their oral side using a 2ml syringe (Dispo van U-40), followed by gentle shaking. The injected urchins were placed in a 1L glass beaker filled with disinfected seawater. The disinfected seawater was prepared by treating the water with 10ppm hypochlorite, then de-chlorinating and filtering it through a 0.2μm cartridge filter. *E. mathaei* began shedding their gametes 40 to 60 seconds after injection. Spermatozoa were released from the dorsal region in the form of a creamy white substance, while the ova were expelled from the aboral side in the form of an orange-colored solution. After the gamete shedding was complete, the urchins were taken out of the beakers, which were then gently rotated in clockwise and anti-clockwise directions for uniform mixing.

The sperms and eggs were collected and moved to a 5L glass beaker containing disinfected seawater for fertilization at room temperature (20 to 25^{o}C). Gentle aeration

was provided, and a black cloth was used to partially cover the beaker to minimize the amount of light entering the container. Free-swimming gastrula stage was obtained after 18 hours and 45 minutes of fertilization and was then transferred to a 20L glass aquarium tank filled with disinfected seawater.

Developmental stages preparation for SEM

After the animals were induced to spawn and the eggs were artificially fertilized, samples were preserved by immersing them in 4% glutaraldehyde in 0.1 M sodium cacodylate buffer (containing 0.1 M calcium chloride and 0.35 M sucrose, with a pH of 7.4) for 48 hours. Following this, the specimens were rinsed three times for 30 minutes each in 0.1 M sodium cacodylate (with 0.4 M sucrose) and then subjected to postfixation with 1% OsO4 in 0.1 M sodium cacodylate buffer for 1 hour. The tissue was dehydrated using a series of ethanol concentrations (30, 50, 70, 85, 95, and 100%), and then subjected to critical point drying using a Tousimis Samdri-795 apparatus. Subsequently, the samples were affixed to aluminum stubs, sputter coated with gold/palladium to a thickness of 5–8nm using a Hummer 6.2, and observed using a JEOL JSM-5300 Scanning Electron Microscope (SEM) operating at 15 to 20 KeV (kilo electron volt) **(Ball & Jangoux, 1990)**.

RESULTS

1. Physico-chemical parameters

Sea water temperature and salinity showed that there were slight differences between them at the two study sites (Table 1). At the second site, there was a low distribution of sea urchins in comparison with the first one. Water turbidity and sedimentation were generally lower at site II than site I. ANOVA single factor test show that there was no significance between temperature at the two study sites ($P = 0.05$), and there was no significance of salinity between the two sites ($P = 0.05$).

Table 1. Seasonal values of the investigated physico-chemical parameters from the two study sites

Season	Temperature (°C)		Salinity (ppt)	
	Mean ± SD		Mean ± SD	
	Site I	Site II	Site I	Site II
Spring 2023	23.34 ± .37	24.65 ± 0.39	39.05 ± 0.11	39.68 ± 0.09
Summer 2023	28.13 ± 0.68	29.56 ± 0.49	40.1 ± 0.04	40.45 ± 0.03
Autumn 2023	25.43 ± 0.45	26.23 ± 0.134	39.25 ± 0.05	39.46 ± 0.05
Winter 2024	18.78 ± 0.39	20.57 ± 0.48	38.67 ± 0.1	38.71 ± 0.1

SD= standard deviation

2. Histological investigation

2.1. Echinometra mathaei gonads

The shell of the sea urchin is internally attached to five gonads. Numerous gonadal acini, which collectively resemble a cluster of grapes, make up each gonadal lobe. Two main cell types are present in each acinus: somatic cells called nutritive phagocytes (NPs), which are present in both male and female sea urchins, and germ cells (GCs), which vary from oogonia to ova in the ovaries and from spermatogonia to fully mature spermatozoa in the testes. These NPs are vital for the storage and provision of nutrients to the GCs during gametogenesis.

Histological examination of gonads define different maturity stages for both sexes. There were four developmental stages for oocytes and spermatocytes observed in *E. mathaei* histological section; Stage I: immature gonad, Stage II: initiation of gametogenesis, stage III: mid of gametogenesis and last stage IV: end of gametogenesis and spawning. This was clear during spring 2023 at the second study sites. Every year, during the reproductive cycle, the gonads of both sexes go through a number of distinct anatomical changes.

Female gametogenesis cycle

Stage I: Immature gonad prior to gametogenesis

This stage lasts for three months, occurring from midwinter to early spring. The ovary post-spawning contains a small number of residual reproductive cells and no nutritive phagocytes (NP) (Fig. 2A). Although residual reproductive cells are present in the female gonads, they appear empty and disorganized. Toward the end of this stage, the number of NP cells increases, and reproductive cells begin to form around the periphery of the gonads. The oocyte diameters measured at the two study sites were 277.48µm ± 14.39 SD and 279.27µm ± 11.94 SD, respectively.

Stage II: Initiation of gametogenesis

A significant presence of developing oocytes is observed at the periphery of the acini, while the gonadal lumen remains filled with NPs (Fig. 2B). This stage lasts for three to four months, from midspring to midsummer. During this time, the size of the reproductive cells increases, and the NPs are utilized. The oocyte diameters during this stage were 341.43µm ± 48.40 SD and 374.93µm ± 65.41 SD for specimens from sites I and II, respectively.

Stage III: Mid-gametogenesis

In this stage, the NPs are utilized and gradually replaced by mature ova in the center of the gonadal lumen. Numerous developing oocytes continue to populate the periphery of the acini, with NPs diminishing in size (Fig. 2C). This stage overlaps with the previous stage until midsummer, peaking during that time as sea water temperatures rise. It lasts five months, from mid-summer to mid-autumn. The oocyte diameters at sites I and II were 475.52µm ± 37.76 SD and 494.33µm ± 37.02 SD, respectively.

Stage IV: End of gametogenesis

By the end of this stage, the gonads are fully mature, with the lumen filled with ripe ova. The periphery of the acini contains shrunken NPs that have lost their nutrient content (Fig. 2D). This stage lasts for three months, from mid-autumn to early winter. Spawning occurs at the end of this stage when all or some reproductive cells are released from the gonads. The oocyte diameters at both study sites were 532.01µm ± 15.9 SD and 535.4µm ± 14.32 SD, respectively. After spawning, the gonadal lumina display numerous empty spaces (Fig. 2E) alongside a few residual ova or spermatozoa. NPs gradually phagocytize the remaining gametes and begin to grow as they accumulate nutrients. After this stage, the gonads revert to stage I, signaling the start of a new reproductive cycle.

Male gametogenesis cycle

Stage I: Immature gonad prior to gametogenesis

This stage lasts for three months, observed from midwinter to early spring. During this period, the male gonadal acini are predominantly filled with NPs (eosinophilic cell populations) (Fig. 3A). Identifying spermatogenic cells in paraffin sections can be challenging; instead, numerous hematoxylin-stained speckles, residues from phagocytized spermatozoa, are frequently noted within the NPs. The peak of this phase occurs in late autumn (post-spawning), indicating that spawning took place in late August and early September. The spermatocyte diameters at both study sites were measured at 99.51µm ± 9.51 SD and 99.44µm ± 9.43 SD.

Stage II: Initiation of gametogenesis

A significant presence of developing clusters of spermatogonia is observed at the periphery of the acini, while the gonadal lumina remain filled with NPs (Fig. 3B). This stage occurs for three to four months, from mid-spring to mid-summer. The spermatocyte diameters at both study sites were 115.97µm ± 15.92 SD and 116.54µm ± 16.74 SD.

Stage III: Mid-gametogenesis

In this stage, NPs are gradually replaced by spermatozoa located in the center of the gonadal lumina. Numerous developing clusters of spermatogonia continue to populate the periphery of the acini, with NPs diminishing in size (Fig. 3C). The peak of this stage is observed in mid-summer, coinciding with an increase in sea water temperature. This stage lasts for three months, from mid-summer to mid-autumn. The spermatocyte diameters were measured at 136.92µm ± 14.76 SD and 137.069µm ± 14.92 SD, respectively.

Stage IV: End of gametogenesis

At the end of this stage, the gonads are fully mature, with their lumina filled with spermatozoa. The periphery of the acini contains shrunken NPs that have lost their nutrient content (Fig. 3D, E). This stage lasts three months, from mid-autumn to mid-winter. Spawning occurs at the end of this stage when all or some of the reproductive cells are released from the gonads (partially spent stage) (Fig. 3F). The spermatocyte diameters at both study sites were measured at 170.38µm ± 21.13 SD and 170.21µm ± 21.42 SD. After spawning, the gonadal lumina display numerous empty spaces along with a few residual spermatozoa. NPs gradually phagocytize the remaining gametes and

begin to grow as they accumulate nutrients. Following this stage, the gonads revert to Stage I, marking the beginning of a new reproductive cycle.

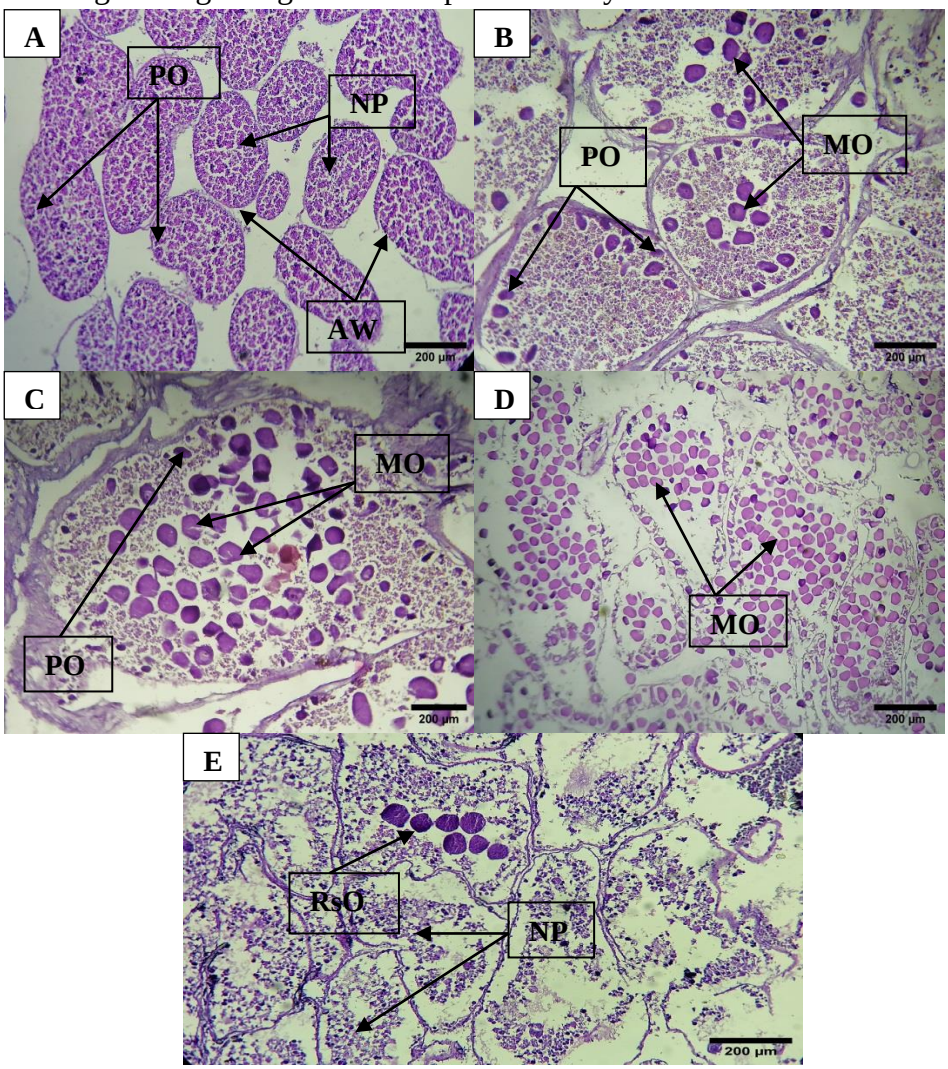

Fig. 2. Histological changes in the ovary of *Echinometra mathaei* during gametogenesis. **(A)** Stage I, **(B)** stage II, **(C)** stage III, **(D)** stage IV and **(E)** Partially spent ovary. NP = Nutritive phagocytes, PO = Previtellogenic ova, MO = Mature ova, Aw = Acinal wall and RsO = Residual ova

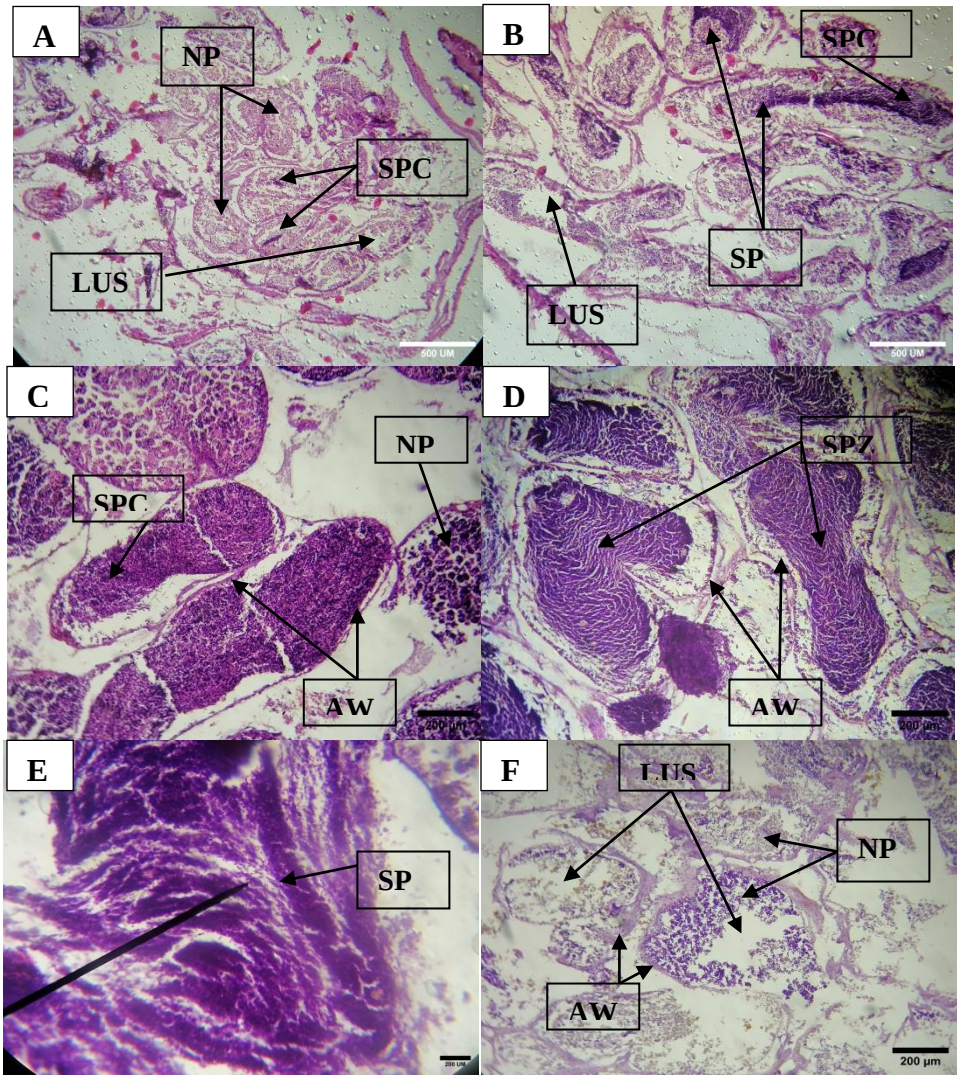

Fig. 3. Histological changes in the testis of *Echinometra mathaei* during gametogenesis. **(A)** Stage I, **(B)** stage II, (C) stage III, (D & E) stage IV, and (F) partially spent testis. SPZ = Spermatozoa, NP = Nutritive Phagocytes, SPC = Spermatocytes, AW = Acinal Wall, LUS = Lumen space and SP = Sperm

3. Induce spawning and Fertilization

E. mathaei demonstrated distinct sexual characteristics and reproduced once a year under specific spawning conditions. Sex determination in sea urchins could not be accurately done through visual inspection; instead, it was based on the color variation of the released gametes (orange eggs and white sperm cloud). The selected samples had similar diameters, with an average test length of 87.66mm and an average weight of 60.8g (Fig. 4). From this result it can concluded that the investigated species is a

broadcasting species, releasing egg and sperms separately and fertilization occurred externally.

The breeders were induced to spawn most effectively through injection with 0.5 mole KCl followed by mechanical shaking. A large proportion of the injected individuals released their gametes within one to five minute, with females producing orange ova and males releasing sperm in a white cloud.

The process of fertilization was highly successful, with a success rate of nearly 100% achieved within a span of 30 minutes. The presence of a complete fertilization membrane surrounding the fertilized ova (zygote) confirmed the occurrence of fertilization. Notably, there were no cases of polyspermy observed. A significant majority, over 95%, of the zygotes progressed to the first cleavage stage, forming 2 cells. Subsequently, the zygotes underwent a series of rapid and complete cleavage cycles to reach the late gastrula stage, a process that took approximately 18 hours and 45mins . The division resulted in the formation of two identical cells with a visible hyaline layer, taking 1 hour and 35 minutes to progress from the zygote stage. The subsequent four-cell stage demonstrated perpendicular orientation of the first and second cleavage cells, requiring approximately two hours and 45 minutes to reach. Following this, the third cleavage led to the development of eight cells after 3 hours and 40min. Subsequent divisions led to the formation of 16 cells, followed by 32, 64, and 128 cell stages, ultimately culminating in the morula stage and to reach to the pervious stages. These take 4 hours and 35 minutes, 5 hours and 30 minutes, 6 hours and 45 minutes and 8 hours and 25 minutes to observe, respectively.

The morula stage consisted of 128 blastomeres. The blastula stage was first detected at 11 and 30 minutes following fertilization. The gastrula stage, on the other hand, manifested as a cell layer encircling a central cavity. Notably, there was a concentration of cells at one end known as the vegetal pole. Gastrulation commenced approximately 12 hours and 25 minutes post-fertilization and the late gastrula was observed after 18 hours and 45 mins. The late gastrula is eventually transformed into a planktonic prismatic stage. This larval form, characterized by a complete digestive system, exhibited a rapid movement and is regarded as an intermediate stage, and this stage completed after 35 hours and 45 minutes. The different developmental stages were photographed by a scanning electron microscope (SEM), as shown in Fig. (5), respectively. The size of different developmental stages and the time to achieve each stage are summarized in Table (2) and Fig. (6).

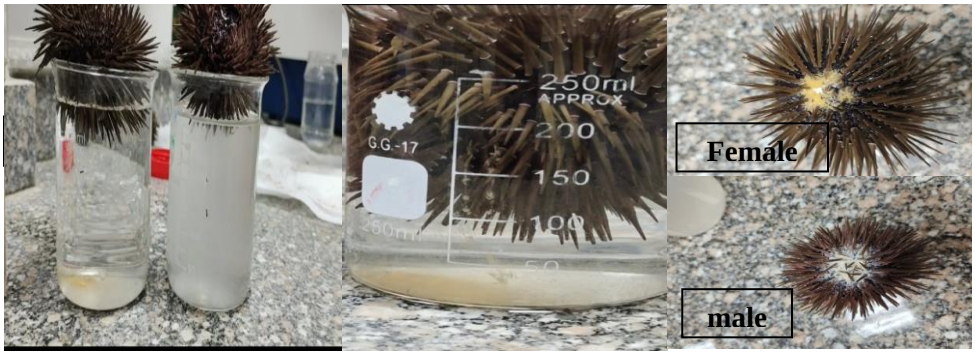

Fig. 4. The induce spawning of *Echinometra mathae*

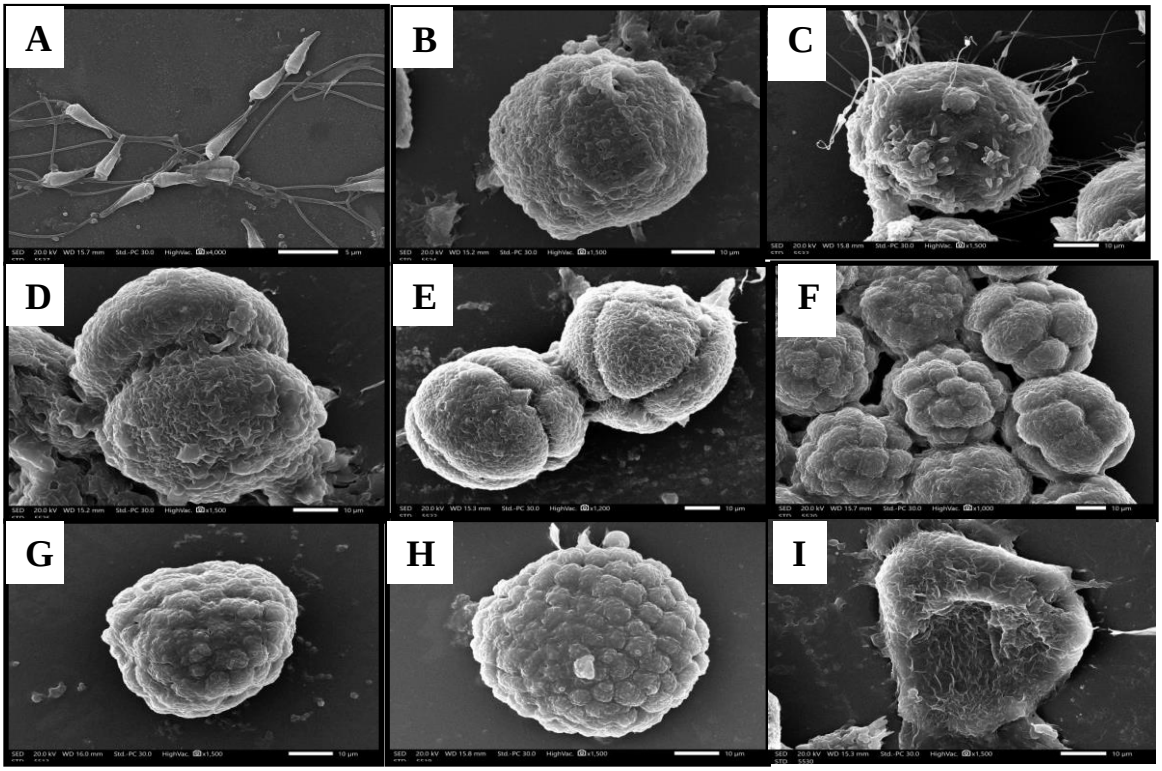

Fig. 5. Different developmental stages by using scanning electron microscope showing: **(A)** Sperm; **(B)** Unfertilized ova; **(C)** Fertilized ova and sperms (zygote); **(D)** First cleavage; **(E)** Second and third cleavages; **(F)** 4^{th}, 5^{th} and 6^{th} cleavages; **(G)** Morula stage; **(H)** Late gastrula stage; and **(I)** The prism stage

Table 2. The mean size of different developmental stages through induce spawning

Developmental stage	Size (µm)	± SD	Time
Unfertilized ova	40.30	0.81	1-2 mins
Fertilized ova (Zygote)	45.34	1.64	30 mins
First cleavage	46.41	2.64	1 hr 35 mins
Second cleavage	49.57	2.18	2 hrs and 45 mins
3rd cleavage	50.43	0.63	3 hrs and 40 mins
4th cleavage	50.99	0.39	4 hrs and 35 mins
5th cleavage	56.22	0.25	5 hrs and 30 mins
6th cleavage	56.37	0.58	6 hrs and 45 mins
Morula stage	56.47	4.54	8 hrs and 25 mins
Blastula stage	58.86	0.32	11 hrs and 30 mins
Gastrula stage	73.06	2.82	18 hrs and 45 mins
Prism stage	80.03	3.54	35 hrs and 45 mins

SD = standard deviation.

4. Effect of some physico-chemical parameters on the maturation of gametes of *E. mathaei*

At the first site, mean sea water temperature (SST) ranged from 23.34ºC in spring to 28.13ºC in summer, while it reached 24.65ºC in spring and 29.56ºC in summer at the second study site. The SST started to decline in autumn to reach 25.43ºC and 26.23ºC at the two study sites, respectively. The minimum SST was recorded in winter (18.78º and 20.57ºC) at the two study sites, respectively.

Salinity was recorded in spring 2023 measuring 39.05 and 39.68ppt at the two study sites, respectively, then started to increase from spring 2023 till it reached the highest value in summer 2023 (40.1 and 40.45ppt, respectively). From the end of summer 2023, the salinity started to decline again to reach 39.25 and 39.46ppt in autumn 2023, while it reached the lowest value in winter 2023, and it was measured to be 38.67 and 38.71ppt. There was a significance between seasons in temperature (P = 0.001).

The predicted maturation time for *E. mathaei* gametes at the two study sites (based on the presence mature gametes) coincided with an increase in SST and the slightly increase of salinity. Between spring 2023 and summer 2023, the SST increased with the increase of salinity. These increase in SST and slightly increase in salinity between spring 2023 and summer 2023 was coincided with an increase in gametes size of target species at both study sites, as the oocytes diameter and spermeries diameters were measured in autumn 2023, and the highest values were 532.01 and 170.377µm and 535.397 and 170.211µm at the two study sites, respectively (Table 3). The predicted spawning time of studied species at the two study sites was based on the subsequently absence of mature

gametes and nutritive phagocytes exhaustion, which occurred in autumn 2023, coinciding with a decline in the three measured environmental parameters. Thus, the slight decrease in temperature and salinity was the favorable conditions for spawning, which was confirmed from the histological sections.

Through applying the extracted data from the two study sites to investigate the interaction between the environmental parameters and their effects on oocytes and spermaries maturation of the burrowing urchin *E. mathaei* by using one way ANOVA test, it appeared that there was a significance between the environmental parameters and maturation of gonads of both sex. A significance was recorded in oocytes and spermaries diameters between seasons, while there was no significance between oocytes and spermaries diameters between the two study sites. Effects of sea water temperature on oocytes and spermaries diameters of *E. mathaei* were highly significant at both study sites (oocytes, $df = 3$, $F = 27.34$, $P = 0.0001$), (spermaries, $df = 3$, $F = 23.9$, $P = 0.0001$) for temperature effect, while for salinity its was (oocytes, $df = 3$, $F = 29.52$, $P = 0.0001$), (spermaries, $df = 3$, $F = 31.81$, $P = 0.0001$).

Table 3. The seasonal mean of oocytes and spermaries diameters of *E. mathaei* at the two study sites with seasonal changes in sea water temperature and salinity

Season	Oocyte diameter SI	Spermary diameter SI	Oocyte diameter SII	Spermary diameter SII	SST SI	SST SII	Salinity SI	Salinity SII
	Mean ± SD	Mean ± SD	Mean ± SD	Mean ± SD	Mean ± SD	Mean ± SD	Mean ± SD	Mean ± SD
Spring 2023	341.43 ± 48.4	115.97 ± 15.92	374.93 ± 65.41	116.54 ± 16.74	23.34 ± 0.37	24.65 ± 0.39	39.05 ± 0.11	39.68 ± 0.09
Summer 2023	475.52 ± 37.76	136.92 ± 14.76	494.33 ± 37.02	137.07 ± 14.92	28.13 ± 0.68	29.56 ± 0.49	40.1 ± 0.04	40.45 ± 0.03
Autumn 2023	532.01 ± 15.9	170.38 ± 21.13	535.4 ± 14.32	170.21 ± 21.42	25.43 ± 0.45	26.23 ± 0.134	39.25 ± 0.05	39.46 ± 0.05
Winter 2024	277.48 ± 14.39	99.51 ± 9.51	279.27 ± 11.94	99.44 ± 9.44	18.78 ± 0.39	20.57 ± 0.48	38.67 ± 0.1	38.71 ± 0.1

SD= standard deviation, SST = sea water temperature

DISCUSSION

The reproductive cycle of most marine invertebrates occurs on an annual basis, with fluctuations in timing noted between locations and from one year to the next one **(Abou Zied, 1991; Hasan, 2019)**.

According to the analysis of gametogenesis, *E. mathaei* exhibited unusual spawning pattern during the period 2023-2024 at the second site (Hurghada), which is characterized by an extended spawning season and recurrent spawning events throughout the year. In contrast, individuals of the target burrowing urchin species demonstrated a distinct annual reproductive cycle, primarily occurring in late summer during the same study period. The observed variations in the mean gonadal index between the two study sites may indicate differences in individual gonadal growth or variations in the synchronization of gonadal development within the population **(Byrne, 1990)**.

Echinoderms at various latitudes exhibit differences in their reproductive patterns. Species found in polar or high-latitude regions show distinct reproductive seasonality **(Grange, 2005)**. The regulation of reproductive activity in echinoderms is influenced by the increasing seasonality as one moves from the tropics to the polar regions **(Byrne *et al.*, 1998)**. This seasonality is absent in tropical species **(Guzmán & Guevara, 2002)** and diminishes in species located in mid-latitudes **(Rubilar *et al.*, 2005)**.

When individuals within a population exhibit synchronization in their growth and maturation processes, any alterations in the average gonadal index will directly correspond to the growth of individual gonads. Consequently, not all stages of maturity will be present throughout the various seasons. Conversely, if gonadal development and maturation occur asynchronously, the population will encompass all stages of maturity at any given time **(Hasan, 2019)**. In the current study, the gondal development and fertilization of *E. mathaei* individuals at the second study site occur asynchronously, as the mature gametes appeared at spring and summer season and lengthen to late autumn season. In contrast to the individuals of the same species, the first time showing asynchronization in both gonadal development and maturity is confirmed by the observation of mature gametes at a specific time through the year from late summer to middle of autumn season (spawning time) during the period 2023-2024. The process of gametogenesis in *E. mathaei* exhibits similarities to that observed in most echinoids, as noted by **Walker *et al.* (2007)**. In the first stage, there is an accumulation of nutrients accompanied by an increase in gonadal size. Following this phase of nutrient accumulation, gametogenic cells begin their growth and maturation along the ovarian wall, coinciding with a reduction in the number of nutritive cells. Ultimately, the mature oocytes and sperm fill the entire lumen of the gonads, leaving minimal nutritive materials. At this stage, any remaining gametes are either reabsorbed or enter a dormant state until the onset of the subsequent reproductive cycle, at which point nutrient

accumulation resumes. **Hellal (1986)** observed that medium-sized oocytes were absent from the gonads post-spawning. In the present study, it was observed that, the medium-sized oocytes were not observed in the individuals of *E. mathaei* at the first study site (Al-Ain, Al-Sukhna, Gulf of Suez), while it was detected in the individuals of the same species at the second study site (Hurghada) during the study period 2023-2024, which is in agreement with the findings of **Hasan (1995, 2019)**.

In the study conducted by **Marcus (2020)**, it was found that sexual maturity sizes varied among species of *Echinometra*. Specifically, *E. lucunter* males were found to reach maturity at 18mm, while females reached maturity at 21mm in diameter; these results align with the current research results as we observed the females reaching maturity at 22mm in diameter. In contrast, individuals of *E. viridis* reached maturity at approximately 15mm in diameter for both sexes. In this context, **Lima *et al.* (2009)** mentioned that the first sexual maturity in *E. lucunter* was observed in individuals with a diameter of at least 20mm. Furthermore, **Drummond (1995)** reported that *E. mathaei* reached first reproduction at a size of 12mm in South Africa.

According to **Cohen-Rengifo *et al.* (2013)**, sea temperatures appear to play a significant role in controlling the periodicities of reproduction as well as fertilization and the early phases of sea urchin growth.

According to **Byrne *et al.* (2009)**, ocean acidification and warming are consequences of global climate change. The study examined how warming and acidification interact to affect the growth and fertilization of this echinoid. For the "business-as-usual" scenario, all combinations of the experimental treatments (20–26°C, pH 7.6–8.2) were tested, with 20°C/pH 8.2 representing ambient conditions. Across all treatments, the fertilization percentage remained high (>89%). Normal development was consistent across all pH levels, but an increase in temperature of +4°C and +6°C resulted in a decrease in cleavage rates by 40 and 20%, respectively, under high-temperature conditions. At +6°C, normal gastrulation dropped below 4%, and development was hindered at 26°C. The findings suggest that while temperature affects sea urchin fertilization and early growth under near-future climate change scenarios, pH does not have a significant impact. In the current study, fertilization and development occurred under normal conditions, showing a high percentage of fertilization and development (>90%).

Energy demand is driven by the availability of food reserves and the amount of energy and resources allocated to reproduction as opposed to other metabolic necessities. This factor serves as a critical determinant in regulating reproductive events, in conjunction with developmental timing factors such as the age and size at sexual maturation. External influences like lunar cycles, salinity, and notably, temperature, also play a significant role in influencing reproduction. Temperature, as a key external factor, impacts a wide range of internal processes, starting from gamete maturation to sexual

maturity and reproductive activities. Water temperature is influenced by various factors, including solar radiation, air temperature, beach radiation, latent heat, and evaporation **(Hasan, 2019)**.

Over the course of the last three decades, the earth's temperature has warmed more than it has in any previous decade since 1850. This warming has been mostly caused by human activity, which has been increasing gradually since the mid-20th century **(IPCC, 2013)**. A trend of steadily rising temperatures over the previous 15 years began in 1995, 1996, and 1997, with respective values of 0.13°C, 0.14°C, and 0.07 [–0.02 to 0.18]°C **(Stocker *et al*., 2013)**. Numerous scholarly works have documented a rise in global temperatures throughout the majority of locations since the early 1980s; the measured warming during the 1971–2010 period varied between 3 and 2°C **(Koven *et al*., 2013)**. The Northern Hemisphere saw its warmest 30-year stretch in the last 1400 years from 1983 to 2012, according to this warming trend. Over 60% of the net energy accumulation within the climate system is retained in the upper layers of the ocean, specifically within the depth range of 0 to 700 meters, while approximately 30% of this energy is contained within the broader oceanic body. As a result, the warming-induced increase in water temperature varies depending on depth, with the upper ocean layer warming more than deeper depths **(Knutti *et al*., 2008)**. Globally, the warming of the ocean is greatly close to the surface; from 1971 to 2010, the upper 75m warmed by 0.11 [0.09 to 0.13]°C every decade. While the temperature increased more slowly between 2003 and 2010 than it did between 1993 and 2002 **(Knutti & Hegerl, 2008; IPCC, 2013)**.

The current study revealed a clear difference between the two study locations in terms of reproductive rhythm, suggesting that the elevated water temperatures at the study sites may have an impact on it. Rises in salinity and surface water temperature were positively correlated with the reproductive cycle. Various researchers demonstrated the presence of significance effect of temperature fluctuations on the reproduction of *E. mathaei* **(Wangensteen *et al*., 2013; Pecorino *et al*., 2014)**. **Bronstein and Loya (2014)** proposed that temperature variation is the primary external signal for *E. mathaei* spawning.

CONCLUSION

It can be concluded that the gametogenesis of *E. mathaei* varies between the two study sites, with synchronization observed at the first site and asynchronization at the second site. The increase in temperature due to global warming has impacted the reproductive cycle of *E. mathaei* in the northern Red Sea.

REFERENCES

Abou Zied, M.M. (1991). Biological studies on some bivalves from the Suez Canal. Ph.D. thesis, Zool. Dept., Faculty of Science, Al-Azhar Univ.

Ahmed, Q.; Ali, Q. M.; Shaikh, I.; Ghory, F. S.; Bat, L.; Mubarak, S. and Baloch, H. (2023). Developmental stages of *Echinometra mathaei* (Blainville, 1825) (Echinodermata-Echinoidea) reared under laboratory conditions from Karachi coast (northern Arabian Sea). *J. Mater. Environ. Sci., 14 (5), 626, 634.*

Ali, A. H. A.; Hamed, M. A. and Abd El-Azim, H. (2011). Heavy metals distribution in the coral reef ecosystems of the Northern Red Sea. *Helgoland marine research*, *65*, 67-80. https://doi.org/10.1007/s10152-010-0202-7.

Andreas, K. (2010). *Echinometra mathaei* (Blainville, 1825). World Echinoidea Database. World Register of Marine Species (WORMS).

Angellia, V. and Nugrahapraja, H. (2023). Study of the sea urchins (echinoidea) influence on the coral reef communities in the Nusa Dua Bali conservation area. *Environmental and Materials*, *1*(1). https://doi.org/10.61511/eam.v1i1.2023.63.

Ball, B. and Jangoux, M. (1990). Ultrastructure of the tube foot sensory-secretory complex in *Ophiocomina nigra* (Echinodermata, Ophiuridea). *Zoomorphology*, *109*, 201-209. https://doi.org/10.1007/BF00312471.

Bronstein, O. and Loya, Y. (2014). Echinoid community structure and rates of herbivory and bioerosion on exposed and sheltered reefs. *J. exp. mar. Biol. Ecol., 456*: 8-17. https://doi.org/10.1016/j.jembe.2014.03.003.

Byrne M.; Andrew, N.L.; Worthington, D.G. and Brett, P.A. (1998). Reproduction in the diadematoid sea urchin *Centrostephanus rodgersii* in contrasting habitats along the coast of New South Wales, Australia. *Marine Biology*. *132*:305–318. https://doi.org/10.1007/s002270050396.

Byrne, M. (1990). Annual reproductive cycles of the commercial sea urchin *Paracentrotus lividus* from an exposed intertidal and a sheltered subtidal habitat on the west coast of Ireland. *Marine Biology*, *104*, 275-289. https://doi.org/10.1007/BF01313269.

Byrne, M.; Ho, M.; Selvakumaraswamy, P.; Nguyen, H. D.; Dworjanyn, S. A. and Davis, A. R. (2009). Temperature, but not pH, compromises sea urchin fertilization and early development under near-future climate change scenarios. *Proceedings of the Royal Society B: Biological Sciences*, *276*(1663), 1883-1888. https://doi.org/10.1098/rspb.2008.1935.

Campbell, A. C. and Gusman, O. (2020). Effect of the south westerly monsoon on seasonal development of *Echinometra mathaei* (de Blainville) at Raaha, Dhofar, Sultanate of Oman. In *Echinoderms through time* (pp. 589-594). CRC Press.

Cohen-Rengifo, M.; Garcia, E.; Hernandez, C.A. and Hernandez C.J. (2013). Global warming and ocean acidification affect fertilization and early development of the sea urchin *Paracentrotus lividus. Cahiers de Biologie Marine*, *54*(4): 132-143.

Drummond, A.E. (1995). Reproduction of the sea urchins *Echinometra mathaei* and *Diadema savignyi* on the South African eastern coast. *Marine and freshwater research*, *46*(4), 751-755. https://doi.org/10.1071/MF9950751.

Grange, L.J. (2005). *Reproductive success in Antarctic marine invertebrates* (Doctoral dissertation, University of Southampton).

Guzmán, H. and Guevara, C. (2002). Annual reproductive cycle, spatial distribution, abundance, and size structure of *Oreaster reticulatus* (Echinodermata: Asteroidea) in Bocas del Toro, Panama. *Marine Biology*, *141*, 1077-1084. https://doi.org/10.1007/s00227-002-0898-2.

Hasan, M.H. (2019). Effect of climate change on the reproduction pattern of sea urchin *Echinometra mathaei* at the Gulf of Suez, Red Sea, Egypt. *Egyptian Journal of Aquatic Biology &Fisheries*, *23*(2), 527-544. DOI: 10.21608/ejabf.2019.35918.

Hasan, M.H. (1995). Ecological and Biological studies on echinoderms from the Gulf of Suez, Red Sea. M.Sc. thesis, faculty of Science, Suez Canal University, 254 pp.

Hellal, A.M. (1986). Biological and ecological studies on some echinoderms of the Red Sea. M.Sc. thesis Faculty of Science, Al-Azhar University.

Hernandez II, E. (2019). Histological evidence of annual and lunar reproductive rhythms of atlantic sea urchin, *Arbacia punctulata* in the Gulf of Mexico: Changes in Nutritive Phagocytes in Relation to Gametogenesis. https://www.proquest.com/dissertations-theses/histological-evidence-annual-lunar-reproductive/docview/2369978342/se-2?accountid=7119.

Hernández, J.C.; Clemente, S. and Brito, A. (2011). Effects of seasonality on the reproductive cycle of *Diadema aff. antillarum* in two contrasting habitats: implications for the establishment of a sea urchin fishery. *Marine Biology*, *158*, 2603-2615. https://doi.org/10.1007/s00227-011-1761-0.

Ibrahim, R. M.; Shaban, W. M.; Ali, A. H. A.; Morsy, G. H. and Abdel-Salam, H. A. (2021). Gametogenic development and synchronous spawning of the acroporid corals Acropora cytherea and Acropora tenuis in the Red Sea. *Egyptian Journal of Aquatic Biology & Fisheries*, *25*(2). https://dx.doi.org/10.21608/ejabf.2021.164595.

IPCC, (2013). Summary for Policymakers. In: Climate Change 2013: The Physical Science Basis. Contribution of Working Group I to the Fifth Assessment Report of the

Intergovernmental Panel on Climate Change [Stocker, T.F., D. Qin, G.-K. Plattner, M. Tignor, S.K. Allen, J. Boschung, A. Nauels, Y. Xia, V. Bex and P.M. Midgley (eds.)]. Cambridge University Press, Cambridge, United Kingdom and New York, NY, USA.

Knutti, R. and Hegerl, G. C. (2008). The equilibrium sensitivity of the Earth‟s temperature to radiation changes. *Nature Geosci., 1*, 735–743. https://doi.org/10.1038/ngeo337.

Knutti, R.; Krähenmann, S.; Frame, D. and Allen, M. (2008). Comment on "Heat capacity, time constant, and sensitivity of Earth‟s climate system"" by S. E. Schwartz. J. Geophys. Res., 113, D15103. https://doi:10.1029/2007JD009473.

Koven, C. D.; Riley, W. J. and Stern, A. (2013). Analysis of permafrost thermal dynamics and response to climate change in the CMIP5 Earth system models. *J. Clim., 26*, 1877–1900. https://doi.org/10.1175/JCLI-D-12-00228.1.

Lima, E. J.; Gomes, P. B. and Souza, J. R. (2009). Reproductive biology of *Echinometra lucunter* (Echinodermata: Echinoidea) in a northeast Brazilian sandstone reef. *Anais da Academia Brasileira de Ciências*, *81*, 51-59. https://doi.org/10.1590/S0001-37652009000100007.

Madhavi, G.; RAO, T. S. C.; Kumar, D. p.; Nagamalleswari, Y. and Sreenu, M. (2000). Histological studies on the endocrine portion of pancreas of the domestic duck (*Anas boschas domesticus*). *Indian Journal of Animal Sciences*, *70*(2), 129-132.

Marcus, N.H. (2020). Phenotypic variability in echinoderms. In *Echinoderm studies 1 (1983)* (pp. 19-37). CRC Press.

Martínez-Pita, I.; García, F.J. and Pita, M.L. (2010). The effect of seasonality on gonad fatty acids of the sea urchins *Paracentrotus lividus* and *Arbacia lixula* (Echinodermata: Echinoidea). *Journal of Shellfish Research*, *29*(2), 517-525. https://doi.org/10.1007/s10152-009-0174-7.

McClanahan, T.R. and Muthiga, N.A. (2020). Echinometra. In *Developments in Aquaculture & Fisheries Science*, *43*, 497-517. Elsevier. https://doi.org/10.1016/B978-0-12-819570-3.00028-7.

Metz, E. C.; Yanagimachi, H. and Palumbi, S. R. (2020). Gamete compatibility and reproductive isolation of closely related Indo-Pacific sea urchins, genus *Echinometra*. In *Biology of echinodermata* (pp. 131-137). CRC Press.

Mortensen, T. (1943). A monograph of the Echinoidea Part III.2, Camarodonta 1. Orthopsidæ, Glyphocyphidæ, Temnopleuridæand, Toxopneustidæ, 553 pp., Copenhagen (C.A. Reitzel).

Nishihira, M.; Sato, Y.; Arakaki, Y. and Tsuchiya, M. (2020). Ecological distribution and habitat preference of four types of the sea urchin *Echinometra mathaei* on the Okinawan coral reefs. In *Biology of echinodermata* (pp. 91-104). CRC Press.

Pearse, J. S. and Cameron, R. A. (1991). Echinodermata: Echinoidea. In: Giese, A. C.; Pearse, J. S.; Pearse, V. B. ed. Reproduction of marine invertebrates. California, The Boxwood Press. Pp. 513-662.

Pecorino, D.; Barker, M. F.; Dworjanyn, S. A.; Byrne, M. and Lamare, M. D. (2014). Impacts of near future sea surface pH and temperature conditions on fertilization and embryonic development in *Centrostephanus rodgersii* from northern New Zealand and northern New South Wales, Australia. *Mar. Biol.*, 161, 101–110. https://doi.org/10.1007/s00227-013-2318-1.

Rashad, M.; Shaban, W.M.; Ali, A.A.M. and Abdel-Salam, H.A. (2020). Reproductive traits and Microstructure of *Acropora digitifera* and *Acropora gemmifera* (Scleractinia, Anthozoa) inhabiting the Northern Red Sea (Hurghada, Egypt). *Egyptian Journal of Aquatic Biology & Fisheries*, *24*(4), 249-266. https://dx.doi.org/10.21608/ejabf.2020.97537.

Rubilar, T.; Pastor de Ward, C.T. and Díaz de Vivar, M.E. (2005). Sexual and asexual reproduction of *Allostichaster capensis* (Echinodermata: Asteroidea) in Golfo Nuevo. *Marine Biology*, *146*, 1083-1090. https://doi.org/10.1007/s00227-004-1530-4.

Siddique, S. and Ayub, Z. (2019). Reproduction of the Sea Urchin *Echinometra mathaei* (Echinoidea: Echinodermata) found on Buleji, rocky coast, Pakistan, North Arabian Sea. *Thalassas: International Journal of Marine Sciences*, *35*, 551-560. https://doi.org/10.1007/s41208-019-0125-2.

Stocker, T.F.; Qin, D.; Plattner, G.-K; Alexander, L.V.; Allen, S.K.; Bindoff, N.L.; Bréon, F. M; Church, .J.A.; Cubasch, U.; Emori, S.; Forster, P.; Friedlingstein, N.; Gillett, J.M.; Gregory, D.L.; Hartmann, E.; Jansen, B.; Kirtman, R.; Knutti, K.; Krishna Kumar, P.; Lemke, J.; Marotzke, V.; Masson-Delmotte, G.A.; Meehl, I.I.; Mokhov, S.; Piao, V.; Ramaswamy, D.; Randall, M.; Rhein, M.; Rojas, C.; Sabine, D.; Shindell, L.D.; Talley, D.G.; Vaughan, D. and Xie, S. P. (2013). Technical Summary. In: Climate Change 2013: The Physical Science Basis. Contribution of Working Group I to the Fifth Assessment Report of the Intergovernmental Panel on Climate Change [Stocker, T.F., D. Qin, G.-K. Plattner, M. Tignor, S.K. Allen, J. Boschung, A. Nauels, Y. Xia, V. Bex and P.M. Midgley (eds.)]. Cambridge University Press, Cambridge, United Kingdom and New York, NY, USA.

Walker, C.W.; Unuma, T. and Lesser, M.P. (2007). Gametogenesis and reproduction of sea urchins. In: Lawrence JM (ed) Edible sea urchins: biology and ecology. Elsevier, Amsterdam, pp 11–33. https://doi.org/10.1016/S0167-9309(07)80066-4.

Wangensteen, O.S; Turon, X.; Casso, M. and Palacin, C. (2013). The reproductive cycle of the sea urchin *Arbacia lixula* in northwest Mediterranean: potential influence of temperature and photoperiod. https://doi.org/10.1007/s00227-013-2303-8.